

# Recent Timing Studies on RXTE Observations of 4U 1538-52

A. Baykal<sup>1</sup>, S.Ç. İnam<sup>2</sup> and E. Beklen<sup>1,3</sup>

<sup>1</sup> Physics Department,

Middle East Technical University, 06531 Ankara, Turkey

altan@astroa.physics.metu.edu.tr

<sup>2</sup> Department of Electrical and Electronics Engineering,

Başkent University, 06530 Ankara, Turkey

inam@baskent.edu.tr

<sup>3</sup> Physics Department,

Süleyman Demirel University, 32260, Isparta, Turkey

elif@astroa.physics.metu.edu.tr

**Abstract.** The high mass X-ray binary pulsar 4U 1538-52 was observed between July 31- August 7, 2003. Using these archival observations, we determined the new orbital epochs for both circular and elliptical orbit models given by Clark (2000). Orbital epochs for both orbit solutions agreed each other and showed that orbital period is constant with  $\dot{P}/P = (0.4 \pm 1.8) \times 10^{-6} \text{ yr}^{-1}$ . Our results are in agreement with those of Clark (2000), in  $1\sigma$  level however give only upper limit for evidence of orbital decay. Determination of pulse frequency showed that the source is still spinning up on average spin up rate  $2.76 \times 10^{-14} \text{ Hz}^{-1}$  since BATSE observations reported by Rubin et al., (1997).

**Key words.** X-rays:binaries; Stars:neutron; pulsars:individual:4U 1538-52; accretion, accretion disks

## 1. Introduction

4U 1538-52 was discovered by Ariel 5 in 1976 with 530s pulsations (Davison, Watson & Pye 1977). A circular orbit with 3.7 day orbital period and 0.51 day long X-ray eclipses were found from the pulse timing (Davison, Watson & Pye 1977; Corbet, Woo & Nagase 1993). The optical companion was found to be the B0 I giant QV Nor (Parkes, Murdin & Mason 1978). Companion's mass was determined to be  $19.8 \pm 3.3 M_{\odot}$  (Reynolds, Bell,

Hilditch, 1992). From the Ginga observations, a cyclotron absorption line near 20 keV was discovered in the X-ray spectrum of 4U 1538-52 which led to a prediction of magnetic field to be  $\sim 1.7 \times 10^{12}$  Gauss (Clark et al. 1990). Detailed modeling of the polar cap structure of 4U 1538-52 was studied with the help of pulse phase spectroscopy (Bulik et al. 1992). BATSE observations of this source permitted the construction of long-term pulse frequency and intensity histories (Rubin, Finger, Scott et al. 1997). Shorter term pulse frequency changes of either sign were observed by BATSE with power density fluctuations in angular acceleration to be consistent with white torque noise on time scales from 16 to 1600 days.

From RXTE observations, Clark (2000) obtained new orbital parameters of the source which led to the evidence of an orbital decay with  $\dot{P}_{orb}/P_{orb} = (-2.9 \pm 2.1) \times 10^{-5} \text{ yr}^{-1}$ . Recent Chandra observations of 4U 1538-52 revealed the presence of a grain-scattered halo around the source (Clark 2004). In this work, using the archival RXTE observations of 4U 1538-52, we present new orbital epoch and pulse frequency measurement.

## 2. Observations

The observations of 4U 1538-52 took place July 31 and August 7, 2003 (MJD 52851 - 52858) with total nominal exposure of  $\sim 75$  ksec. The results presented here are based on data collected with the Proportional Counter Array (PCA, Jahoda et al., 1996). The PCA instrument consists of an array of five collimated xenon/methane multianode proportional counters. The total effective area is approximately  $6250 \text{ cm}^2$  and the field of view is  $\sim 1^0 \text{ FWHM}$  and a nominal energy range extending from 2 to 60 keV.

## 3. Determination of Orbital Epoch and Pulse Frequency

Background light curves and X-ray spectra were generated by using background estimator models based on the rate of very large events (VLE), detector activation, and cosmic X-ray emission. The background lightcurves were subtracted from the source light curve obtained from the binned Good Xenon data. In Figure 1, we present the background subtracted lightcurve. For the timing analysis, we corrected the lightcurve to the barycenter of the solar system. We also corrected the barycentered light curves for binary orbital motion using both circular and elliptical orbital models given by Clark (2000). Then a template pulse profile was created by folding all light curves into one master pulse. In order to find the pulse frequency, and new orbital epoch, we obtained 13 pulse arrival times through the  $\sim 2$  binary orbit using cross correlation technique. Each individual pulse profile (one pulse arrival time for each RXTE orbit) were found by folding the light curve into one average for each RXTE orbit.

In the pulse timing analysis, we used the method of harmonic representation of pulse profiles, which was proposed by Deeter & Boynton (1985). In this method, pulse profiles

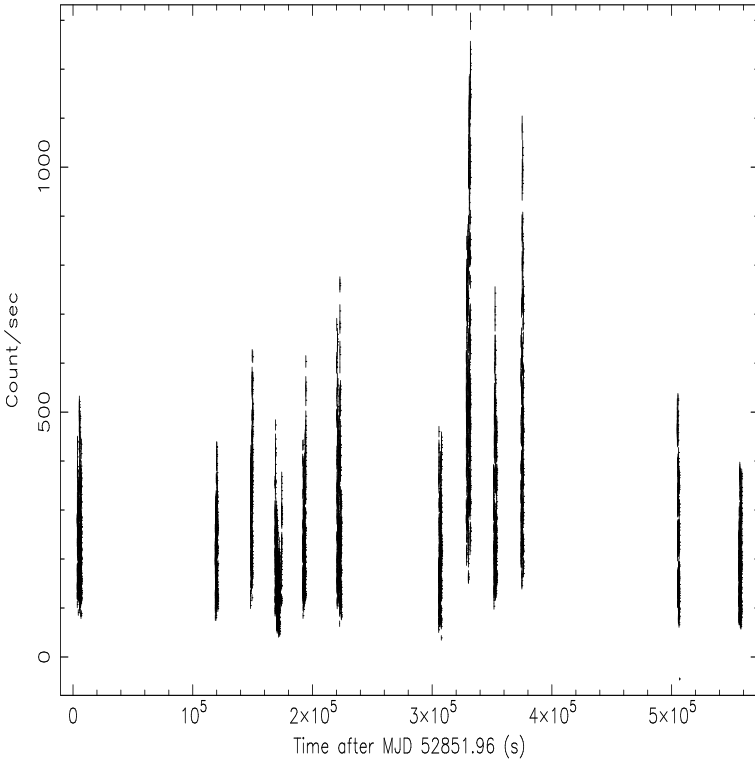


Fig. 1 – 2-30 keV RXTE-PCA lightcurve of 4U 1538-52

are expressed in terms of harmonic series and cross-correlated with the template pulse profile. The maximum value of the cross-correlation is analytically well-defined and does not depend on the phase binning of the pulses. The master pulse with 20 phase bins was represented by their harmonics (Deeter & Boynton 1985) and cross-correlated with harmonic representations of the pulse profiles from segments of the data.

HMXRB source 4U 1538-52 have variable pulse profiles which affects the pulse timing. In order to estimate the errors in the arrival times, the light-curve of each RXTE orbit was divided into approximately 4-5 equal subsets and new arrival times were estimated. The average variance in the arrival times of all RXTE orbits were computed and treated as errors of arrival times.

The residual pulse arrival times may arise from the change of the pulse frequency during the observation (or intrinsic pulse frequency derivative) and from the errors of orbital parameters (Deeter et al., 1981),

$$\delta\phi = \phi_o + \delta\nu(t - t_o) + \frac{1}{2}\dot{\nu}(t - t_o)^2 - \nu \frac{2\pi\delta T_{\pi/2} \sin i}{P_{\text{orbit}}} \cos l_n \quad (1)$$

where  $\delta\phi$  is the pulse phase offset deduced from the pulse timing analysis,  $t_o$  is the mid-time of the observation,  $\phi_o$  is the phase offset at  $t_o$ ,  $\delta\nu$  is the deviation from the mean pulse frequency (or additive correction to the pulse frequency), and  $\dot{\nu}$  is the pulse frequency derivative of the source,  $T_{\pi/2}$  is the epoch when the mean orbital longitude is equal to 90 degrees,  $P_{\text{orbit}}$  is the orbital period,  $\delta$  denotes the errors of these parameters,  $l_n = 2\pi(t_n - T_{\pi/2})/P_{\text{orbit}} + \pi/2$  is the mean orbital longitude at  $t_n$ . The above expression

was fitted to the pulse arrival times data for both circular and elliptical orbit model given by Clark (2000). In this method, we determined the orbital epoch and intrinsic pulse frequency derivative for circular and elliptical orbit models. In Table 1, we present orbital epoch based on both circular and elliptical orbits, and intrinsic pulse frequency derivatives for both circular and elliptical orbital models and pulse frequency. As it is seen from Table 1, orbital epochs for both models agree each other in  $1\sigma$  level. In order to compare our technique with the published orbital epochs, we extracted observations in 1997 (MJD 50449.93-50453.69) and estimated orbital epochs for these observations. We confirmed orbital epochs given by Clark (2000). In Figure 2, we present best fit and residuals of arrival times. In Table 1, we present the orbital epochs and phases of orbital epochs from a fitted linear function of orbit number are shown in Figure 3. A quadratic fit to the epochs from all experiments yielded an upper limit of orbital period change as  $\dot{P}_{orb}/P_{orb} = (0.4 \pm 1.8) \times 10^{-6} \text{ yr}^{-1}$ . In Figure 4, we display long term pulse frequency of the source.

**Table 1.** Orbital Parameters of 4U 1538-52/QV Nor Binary System<sup>a</sup>

Parameter	Elliptical Orbit	Circular Orbit
$a_x \sin i$ (lt-s)	$56.6 \pm 0.7$	$54.3 \pm 0.6$
$T_{\pi/2}$ (MJD)	$52855.0421 \pm 0.025$	$52855.0441 \pm 0.025$
$P_{pulse}$ (s)	$526.8551 \pm 0.016$	$526.8535 \pm 0.013$
$\dot{\nu}$ (Hz s $^{-1}$ )	$(2.838 \pm 4.124) \times 10^{-13}$	$(2.241 \pm 2.764) \times 10^{-13}$
$\chi^2$ ( $\sigma_p = 1.92$ sec)	1.44	1.0

(<sup>a</sup> Orbital parameters are taken from Clark (2000))

#### 4. Discussion

Before CGRO observations, 4U 1538-52 had been found to have a long term spin down trend. A linear fit to pre-CGRO pulse frequency history gives  $\dot{\nu}/\nu \sim -8 \times 10^{-12} \text{ s}^{-1}$  and linear fit to CGRO and our RXTE result yields  $\dot{\nu}/\nu \sim 1.45 \times 10^{-11} \text{ s}^{-1}$ . At longer time spans this corresponds to spin up/down transitions at the order of 3000-4000 yrs. Rubin et al (1997) constructed the power spectrum of pulse frequency derivative fluctuations. Their analysis showed that pulse the frequency derivative fluctuations can be explained on timescales from 16 to 1600 days with an average white noise strength of  $(7.6 \pm 1.6) \times 10^{-21} (\text{Hz s}^{-1})^2 \text{ Hz}^{-1}$ . A random walk in pulse frequency (or a white noise in pulse frequency derivative) can be explained as a sequence of sudden steps in pulse frequency  $\langle \delta\nu^2 \rangle^2$  which occurs at a constant rate R. Then the RMS variation of pulse frequency variations can be scaled in elapsed time  $\tau$  as  $\langle \Delta\nu^2 \rangle = R \langle \delta\nu^2 \rangle \tau$  (Hz), where  $S = R \langle \delta\nu^2 \rangle$  is defined as noise strength. Then, RMS scaling for the pulse frequency derivatives can be obtained as  $\langle \Delta\nu^2 \rangle = (S/\tau)^{1/2}$ , Hz s $^{-1}$ . As seen from Table 1, in

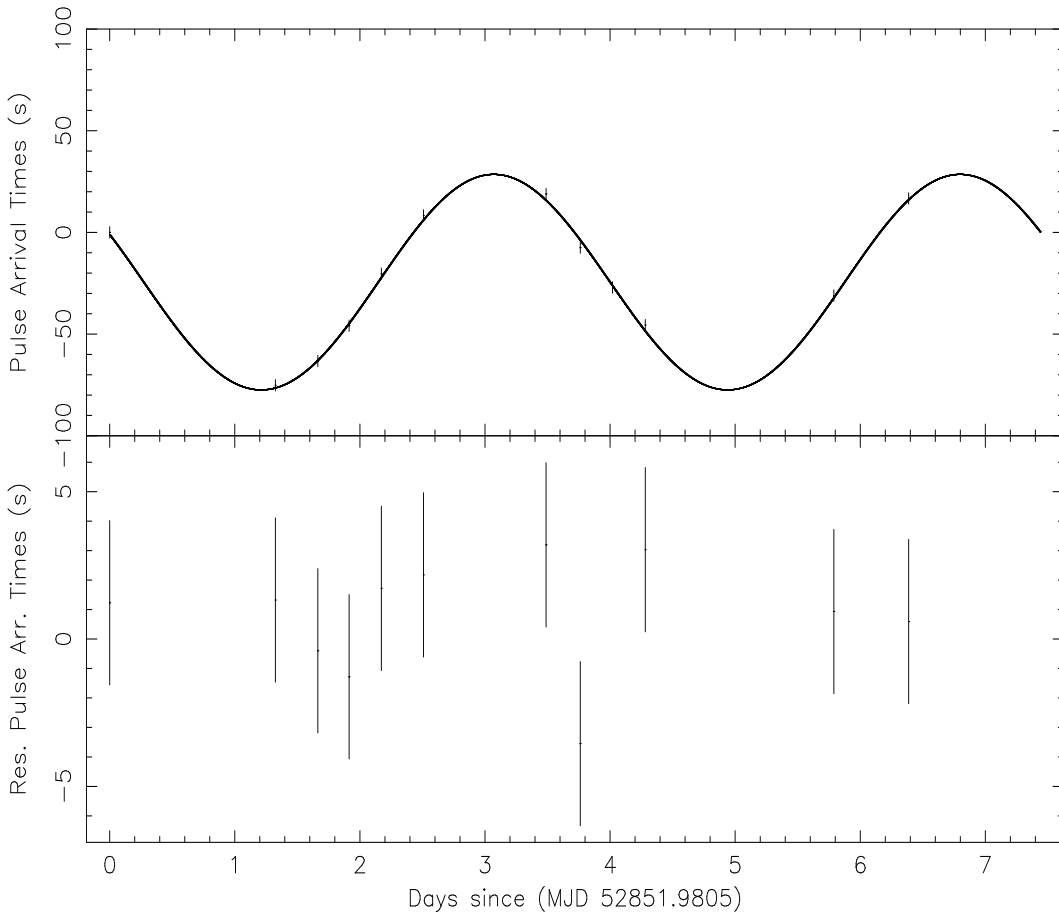


Fig. 2 – **(top)** Pulse arrival times and best fitted elliptical orbital model given by Clark (2000). **(bottom)** Residuals removing best orbital model. Note that reduced  $\chi^2$  equals 1 for uncertainty in arrival times equals 1.92 seconds.

our fits, upper limits of intrinsic pulse frequency derivatives are 7-10 times higher than the long term spin up rates. If white noise in pulse frequency can be interpolated to a few days, then the upper limits in the change of pulse frequency derivatives in a week should be  $< \Delta \dot{\nu}_{\text{week}}^2 > / < \Delta \dot{\nu}_{\text{1600days}}^2 > = (1600/7)^{1/2} = 15$ . Therefore the higher values of upper limits of pulse frequency derivatives obtained in our fits (see Table 1) are consistent with the statistical nature of the white noise in pulse frequency derivatives observed in this source.

Previous measurement of change in the orbital period,  $(-2.9 \pm 2.1) \times 10^{-6} \text{ yr}^{-1}$  (Clark 2000), and our new value for the orbital period change,  $\dot{P}/P = (0.4 \pm 1.8) \times 10^{-6} \text{ yr}^{-1}$ , are consistent with zero in  $1\sigma$  error range. As seen from Figure 2, our orbital epoch period is consistent with previous BATSE, Ginga measurements and  $1\sigma$  different from recent RXTE measurement by Clark (2000).

There two major ways in which the orbital angular momentum of a binary system may change (Kelley et al. 1983). The first possible way involves the loss of mass from at least one of the binary components which may, for instance, happen in case of accretion

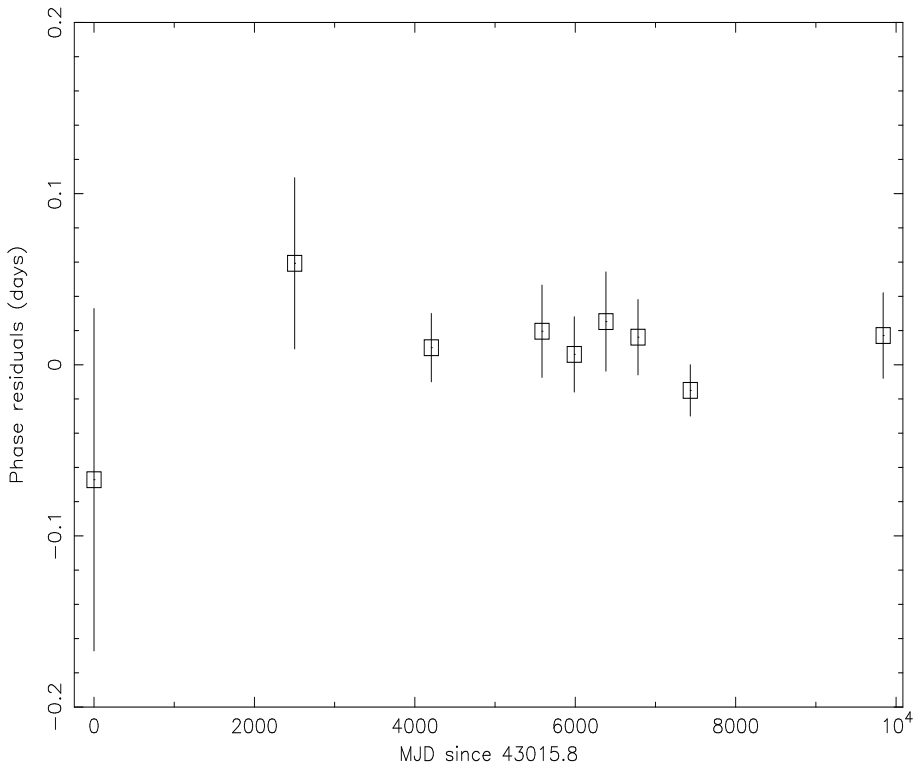


Fig. 3 – Overall orbital epoch for 4U 1538-52. The rightmost point corresponds to most recent RXTE observation of ID 80016.

due to Roche lobe overflow of a companion or by virtue of a strong stellar wind of at least one of the companions. Even if the total mass and total angular momentum of the system is conserved, the orbital period may still change due to the redistribution of the angular momentum. If the mass is lost in the binary system, the lost mass probably carries away the angular momentum of the system. Another possible way of a change in angular momentum of a binary system is through a tidal interaction. The tidal interaction of the binary system results in a torque which tends to decrease or increase the orbital angular momentum of the system as in the case of increasing orbital period in the Earth-Moon system (Counselman 1973).

In most of the X-ray binaries with accretion powered pulsars, the evolution of the orbital period seems to be too slow to be detectable. Yet there are still some such systems in which this evolution was measured and  $\dot{P}/P$  were reported. These systems include Cen X-3 with  $(-1.8 \pm 0.1) \times 10^{-6} \text{ yr}^{-1}$  (Kelley et al. 1983; Nagase et al. 1992), Her X-1 with  $(-1.32 \pm 0.16) \times 10^{-8} \text{ yr}^{-1}$  (Deeter et al. 1991), SMC X-1 with  $(-3.36 \pm 0.02) \times 10^{-6} \text{ yr}^{-1}$  (Levine et al. 1993), Cyg X-3 with  $(1.17 \pm 0.44) \times 10^{-6} \text{ yr}^{-1}$  (Kitamoto et al. 1995), 4U 1700-37 with  $(3.3 \pm 0.6) \times 10^{-6} \text{ yr}^{-1}$  (Rubin et al. 1996), and LMC X-4 with  $(-9.8 \pm 0.7) \times 10^{-7} \text{ yr}^{-1}$  (Levine et al. 2000). Change in the orbital period of Cyg X-3 was associated with the mass loss rate from the Wolf-Rayet companion star. For 4U 1700-37, the major cause of orbital period change was also thought to be mass loss from

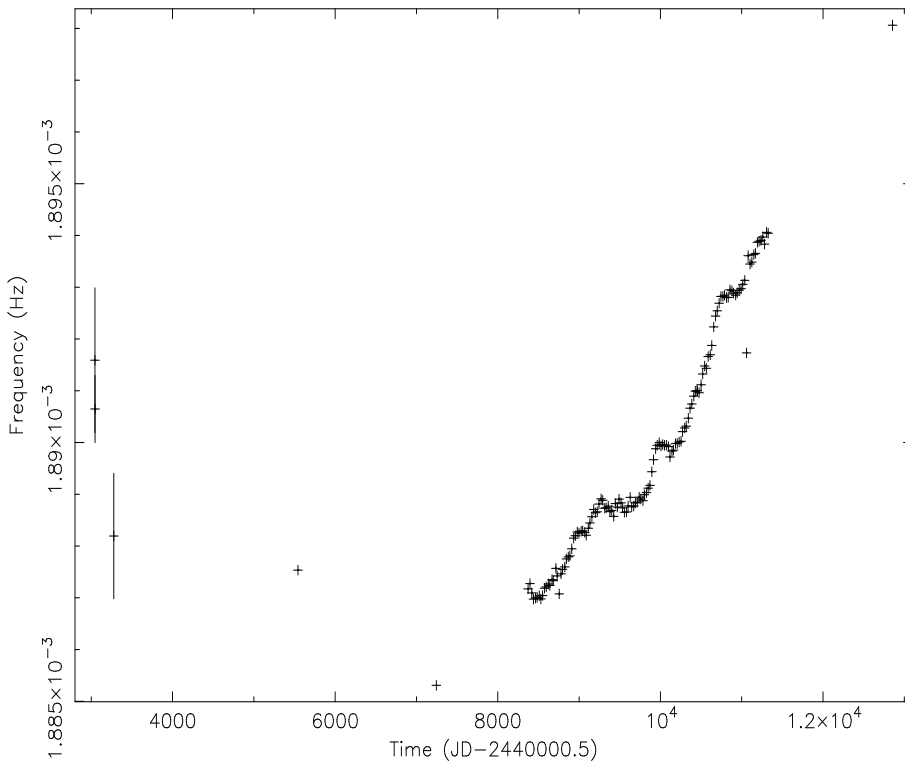


Fig. 4 – Pulse frequency history of 4U 1538-52

the companion star. For Her X-1, mass loss and mass transfer from the companion was proposed to be the major factors changing the orbital period of the system. Extended low states of Her X-1 in which mass loss increases significantly may also have important effect on the variation of the orbital period.

On the other hand, for the high mass X-ray binary systems Cen X-3, LMC X-4 and SMC X-1, the major cause of change in the orbital period is likely to be tidal interactions (Kelley et al. 1983; Levine et al. 2000; Levine et al. 1993). For these three systems, orbital period decreases (i.e. derivative of the orbital period is negative). Our new measurements of orbital period change gives new upper limit at order of  $\dot{P}/P = -10^{-6} \text{ yr}^{-1}$  which is similar to the observed values of SMC X-1 and Cen X-3. The upper limits of possible orbital decay should at the same order for 4U 1538-52. Further observations can give further information about the orbital period change of this source.

## References

- Bulik, T., Meszaros, P., Woo, J.W., Nagase, F., Makishima, K., 1992, ApJ, 395, 564
- Clark, G.W., Woo, J.W., Nagase, F. et al. 1990, ApJ, 353, 274
- Clark, G.W. 2000, ApJL, 542, 133
- Clark, G.W. 2004, ApJ, 610, 956
- Corbet, R.H.D., Woo, J.W., Nagase, F. 1993, A& A, 276, 52
- Counselman, C.C. 1973, ApJ, 180, 307

Davison, P.J.N., Watson, M.G., Pye, J.P. 1977, MNRAS, 181, 73

Deeter, J.E., Boynton, P.E., Pravdo, S.H. 1981, ApJ, 247, 1003

Deeter, J.E., Boynton, P.E. 1985, in Proc. Inuyama Workshop on Timing Studies of X-ray Sources, ed. S. Hayakawa& F.Nagase (Nagoya: Nagoya Univ.), 29

Deeter, J.E., Boynton, P.E., Miyamoto, S. et al. 1991, ApJ, 383, 324

Jahoda, K., Swank, J.H., Giles, A.B., Stark, M.J., Strohmayer, T., Zhang, W., Morgan, E.H., 1996, Proc. SPIE, 2808, 59

Kelley, R.L, Rappaport, G., Clark, G.W., Petro, L.D. 1983, ApJ, 268, 790

Kitamoto, S., Hirano, A., Kawashima, K. et al. 1995, PASJ, 47, 233

Levine, A., Rappaport, S., Deeter, J.E. et al. 1993, ApJ, 410, 328

Levine, A.M., Rappaport, S.A., Zojcheski, G., 2000, ApJ, 541, 194

Nagase, F., Corbet, R.H.D., Day, C.S.R., et al. 1992, ApJ, 396, 147

Parkes, G.E., Murdin, P.G., Mason, K.O. 1978, MNRAS, 184, 73

Reynolds, A.P., Bell, S.A., Hilditch, R.W. 1992, MNRAS, 256, 631

Rubin B.C. et al. 1996, ApJ, 459, 259

Rubin, B.C., Finger, M.H., Scott, D.M. et al. 1997, ApJ, 488, 413